X-921-77-142
PREPRINT

Tmx 71361

FAULTING PARAMETERS DERIVED FROM COMPUTER SIMULATION OF EARTHQUAKES

(NASA-TM-X-71361) FAULTING PARAMETERS DERIVED FROM COMPUTER SIMULATION OF EARTHQUAKES (NASA) 29 p HC A03/MF A01 CSCL 08K
N77-30681
Unclas
G3/46 42858

STEVEN C. COHEN

JUNE 1977

GSFC
GODDARD SPACE FLIGHT CENTER
GREENBELT, MARYLAND

X-921-77-142
Preprint

FAULTING PARAMETERS DERIVED FROM COMPUTER SIMULATION OF EARTHQUAKES

Steven C. Cohen
Geodynamics Branch

June 1977

GODDARD SPACE FLIGHT CENTER
Greenbelt, Maryland

FAULTING PARAMETERS DERIVED FROM COMPUTER SIMULATION OF EARTHQUAKES

Steven C. Cohen

ABSTRACT

The interrelationships among the seismic source parameters average displacement, rupture length, and strain energy release are investigated by computer simulation using a coupled massive block model of the sliding along an active fault. Average displacements and energy release vary considerably with the degree of heterogeneity in the friction and elastic parameters used in the model. With high heterogeneity in either parameter, average displacement rises more rapidly with rupture length for short ruptures than for longer ones. Strain energy release is determined primarily by the product of dynamic friction, rupture length, and average displacement. The observed interrelationships among the faulting parameters are for the most part, consistent with theoretical arguments and experimental data. By contrast the variation in the frequency of occurrence of simulation events with strain energy release is somewhat different from the variation in the frequency of naturally occurring events with seismic energy.

Page intentionally left blank

CONTENTS

ILLUSTRATIONS

ILLUSTRATIONS (Continued)

FAULTING PARAMETERS DERIVED FROM COMPUTER SIMULATION OF EARTHQUAKES

INTRODUCTION

Computer simulation is a convenient tool for investigating various hypotheses concerning earthquake mechanics and for exploring the correlations that exist among the source parameters. Recently we reported (Cohen, 1976, 1977) how the pattern of simulation events varies with the distribution of elastic, viscous, and friction constants in Dieterich's (1972) elastic and viscoelastic models. In this paper we present, for the elastic model, data on the correlations among the average displacement, rupture length, and strain energy release. We also examine the frequency of occurrence of events with varying strain energy release.

The basic features of the elastic model are shown in Figure 1. An active strike slip fault is represented by a set of coupled mechanical blocks which are driven along a friction surface by the coupling to a moving plate. The elastic constants and the friction strengths may vary from block to block. As the driving plate moves to the right, tension accumulates in the driving springs until the frictional strength holding one of the blocks in place is exceeded. The block begins to slide thereby increasing the stress in the connecting springs and possibly stimulating the adjacent blocks into motion. Events of varying magnitude, displacement, and rupture length are generated. The spatial-temporal pattern of events is strongly affected by the form of the friction and elastic constant distributions. The details of the system behavior are discussed by Dieterich (1972) and Cohen (1976, 1977).

The correlations and statistical features which we present in this paper are derived from three representative simulations which are summarized in Figure 2. In simulation EL-I, the static friction varies by a factor of 3 in a random manner with a mean value of 2×10^{20} dynes. The elastic constants are uniform. By contrast in EL-II there is only a very small heterogeneity in the friction parameter, ±2.5 percent at most, and again there is homogeneity in the elastic constants. In EL-III the friction is uniform but the elastic constants vary by a factor of 3. We turn now to an examination of the interrelationships among the simulation source parameters.

Average Displacement Versus Rupture Length

The average displacement, Δx, versus rupture length (number of blocks, N, displaced in the event) is plotted for EL-I in Figure 3. For N less than four, the mean average displacement rises with increasing rupture length. In this region block displacement is enhanced by simultaneous motion in the adjacent blocks which reduces the restraining forces due to a compression of the connecting springs. For N greater than three or four, the mean average displacement shows little further sensitivity to the length of the rupture as the displacement of a block is only indirectly affected by motion in more distant than nearest neighbors.

The more homogeneous nature of EL-II manifests itself in a reduced sensitivity of average displacement to rupture length as shown in Figure 4. Not only is the mean average displacement less sensitive to rupture length, but also the spread of average displacements values for a fixed rupture length is greatly reduced over those for EL-I. The standard deviations in the average displacements range from about 40 cm (N = 7) to over 105 cm (N = 1) for EL-I, but are in the range 4-10 cm for EL-II.

The heterogeneity in the spring constants of EL-III produces less sensitivity in the mean average displacement versus rupture length than does the heterogeneity in the friction parameter in EL-I. The results for EL-III are shown in Figure 5, and the contrast between the behavior of EL-I and EL-III might be attributable to the fact that both the friction and driving spring directly affect only one block while the connecting spring directly affects two blocks.

<u>Strain Energy Versus Rupture Length</u>

The strain energy released in the simulation events are shown as a function of rupture length in Figures 6 through 8. For EL-I the mean average energy rises faster than linear with rupture length for small numbers of moving blocks and approaches linearity for $N > 3$. For EL-II we find $E \sim N$ throughout the range of observed rupture lengths. These results can be explained by considering the relationship between strain energy release and dynamic friction, f^d displacement, and rupture length:

$$E = \sum_i \int f_i^d \, dx_i = \sum_i f_i^d \, \Delta x_i = N < f^d \Delta x > \quad (1)$$

where the sum over the N blocks moving in the event. Therefore to the extent that $<f^d \Delta x>$ is independent of rupture length, $E \sim N$. For EL-I this is a fair approximation for $N > 3$. For EL-II the near uniformity in the friction distributions and the previously shown insensitivity of the average displacement to rupture length make the assumption a good one. For EL-III f^d is unvarying but $<\Delta x>$ does increase with N. We find for this particular case, $E \simeq N^{1.2}$.

Strain Energy Release Versus Average Displacement

We show in Figures 9 and 10 the dependence of the released strain energy on average displacement for EL-I and EL-III respectively. (Because of the restricted range of average displacements for EL-II, the results for this case are not shown.) The data suggest

$$\log E \simeq A + B \log < \Delta x > \quad (2)$$

where both A and B can depend on the number of blocks moving in the event. In the case of EL-I, for $N = 1$, $B = 2$, and the relationship is exact. For $N > 2$ the relationship is approximate and B approaches 1 as N increases. In the case of EL-III the relationship is also exact and $B = 1$. These results are explained theoretically in the next section.

Strain Energy Release Versus Product of Rupture Length and Average Displacement

Several of the results of the previous sections can be explained in a convenient manner by considering the variation in strain energy release with the product of rupture length and average displacement. The results are shown in Figures 11 through 13 which we discuss with the help of arguments presented by King and Knopoff (1968). They show that the strain energy released in an event is related to the average of pre- and post-event force on the block, $\overline{F}_i$, and the displacement by

$$E = \sum_i \overline{F}_i \, \Delta x_i \tag{3}$$

For EL-I and N = 1, a simple calculation shows $\overline{F} = f^d \sim \Delta x$, hence $E \sim \Delta x^2$ as confirmed by the data. In another case we suppose the $\overline{F}_i$'s can be removed from under the summation sign and replaced by a representative value, then

$$E = \overline{F} \sum_i \Delta x_i = \overline{F} N < \Delta x > \tag{4a}$$

or

$$\log E = \log \overline{F} + \log N < \Delta x > \tag{4b}$$

For EL-I, $N > 3$ and for EL-II, all N, this approximation is a good one as the data show. For EL-III the relationship is exact. Comparing Equations (2) and (4b) we see $A = \log N + \log \overline{F}$, $B = 1$.

Frequency of Occurrence Versus Strain Energy Release

A well established relationship for the frequency of occurrence, $\mathscr{F}$, of seismic events of magnitude less than or equal to M is

$$\log \mathscr{F} = a - bM \tag{5}$$

Some deviations from this simple relationship are pronounced for very large and very small events. We wish to discover whether a similar relationship can be established for the frequency and logarithm of strain energy release in simulation events. The data shown in Figure 14 reveal marked departure from this simple behavior. This is in contrast to the results of King (1975) who uses a mechanical model somewhat similar to our computer simulator. He finds Equation (5) fits his data reasonably well with M replaced by the logarithm of the strain energy released. Although there are some differences between the mechanical and computer simulator models, we are not sure of the origin of these different results.

CONCLUSIONS

In this paper we have used computer simulation techniques to study the correlations among the seismic source parameters. We summarize the central conclusions by model.

EL-I – heterogeneous friction – average displacement initially rises with rupture length, then becomes insensitive to further increases for longer rupture lengths; significant variations in average displacement and energy released in different events with same rupture length; strain energy release rises as square of average displacement for single block ruptures and approaches a linear dependence on the product of rupture length and average displacement as the length increases.

EL-II - slight friction heterogeneity, otherwise uniform - average displacement only weakly sensitive to length with little variation among events with common rupture lengths; strain energy release increases linearly with rupture length-average displacement product and hence approximately linearly with rupture length.

EL-III - heterogeneous elasticity - average displacement increases with rupture length although rise less rapid at small rupture lengths than for EL-I, strain energy release is determined by product of dynamic friction, number of blocks in rupture, and average displacement.

In all three simulations there is considerable deviation from a linear relationship between the logarithm of event frequency and the logarithm of strain energy release.

REFERENCES

Cohen, S. C., Computer Simulation of Earthquakes, NASA/GSFC X-921-76-258, Goddard Space Flight Center, 1976.

Cohen, S. C., Computer Simulation of Earthquakes, J. Geophys. Res., in press.

Dieterich, J. H., Time Dependent Friction as a Possible Mechanism for Aftershocks, J. Geophys. Res., 77, 3771-3781, 1972.

King, C. Y and L. Knopoff, Model Seismicity: Rupture Parameters, Stress and Energy Relations, J. Geophys. Res., 73, 1399-1406, 1968.

King, C. Y., Model Seismicity and Faulting Parameters, Bull. Seismol. Soc. Amer., 65, 245-259, 1975.

FIGURE CAPTIONS

Figure 1. Mechanical block representation of fault

Figure 2. Description of the models used in the computer simulations

Figure 3. Average displacement versus rupture length for EL-I. The X's represent mean values and the bars show the range for one standard deviation about the mean.

Figure 4. Average displacement versus rupture length for EL-II. The standard deviations are too small ($<$ 10 cm) to show on the figure.

Figure 5. Average displacement versus rupture length for EL-III

Figure 6. Energy versus rupture length for EL-I. The X's represent mean values of log E and the bars show the range for one standard deviation about the mean.

Figure 7. Energy versus rupture length for EL-II. The standard deviations are too small ($\leqslant$ 0.01) to show on the figure.

Figure 8. Energy versus rupture length for EL-III

Figure 9. Energy versus average displacement for EL-I. Each point represents at least one event.

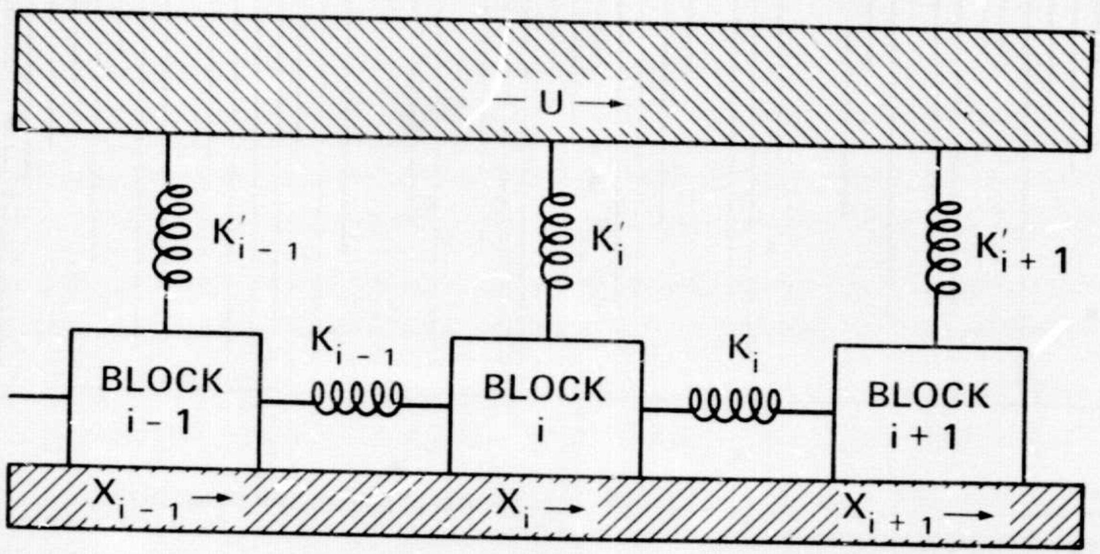

Figure 1. Mechanical block representation of fault

MODEL	DESCRIPTION
EL I	STATIC FRICTION RANDOMLY DISTRIBUTED IN RANGE 1×10^{20} - 3×10^{20} DYNES DRIVING SPRING ELASTIC CONSTANT = 1×10^{17} DYNES/CM - ALL SPRINGS CONNECTING SPRING ELASTIC CONSTANT = 5×10^{16} DYNES/CM - ALL SPRINGS
EL II	STATIC FRICTION RANDOMLY DISTRIBUTED IN RANGE 1.95×10^{20} - 2.05×10^{20} DYNES DRIVING SPRING ELASTIC CONSTANT = 1×10^{17} DYNES/CM - ALL SPRINGS CONNECTING SPRING ELASTIC CONSTANT = 5×10^{16} DYNES/CM - ALL SPRINGS
EL III	STATIC FRICTION = 2×10^{20} DYNES DRIVING SPRING ELASTIC CONSTANT RANDOMLY DISTRIBUTED IN RANGE 5×10^{16} - 1.5×10^{17} DYNES/CM CONNECTING SPRING CONSTANT BETWEEN BLOCK i AND BLOCK i + 1 = ONE-HALF VALUE OF DRIVING SPRING CONSTANT FOR BLOCK i.

IN ALL MODELS DYNAMIC FRICTION = 4/5 STATIC FRICTION. THE RANDOM DISTRIBUTIONS USED IN THE MODELS ARE SHOWN BELOW.

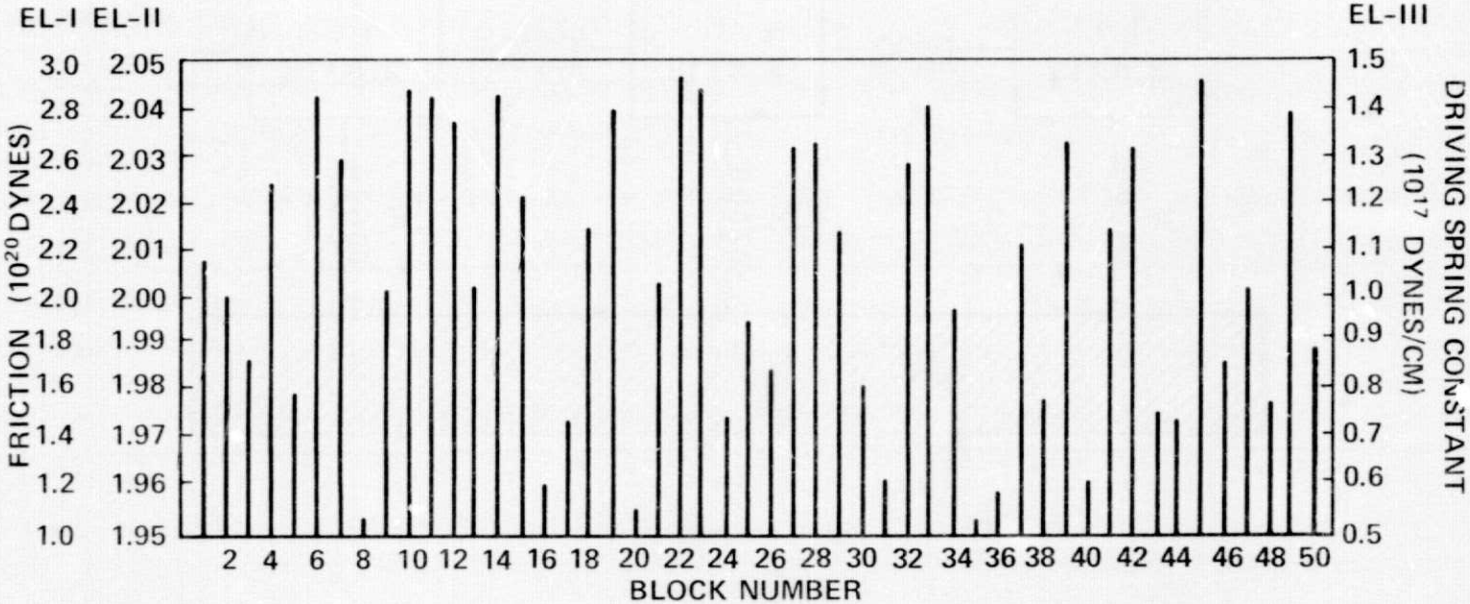

Figure 2. Description of the models used in the computer simulations

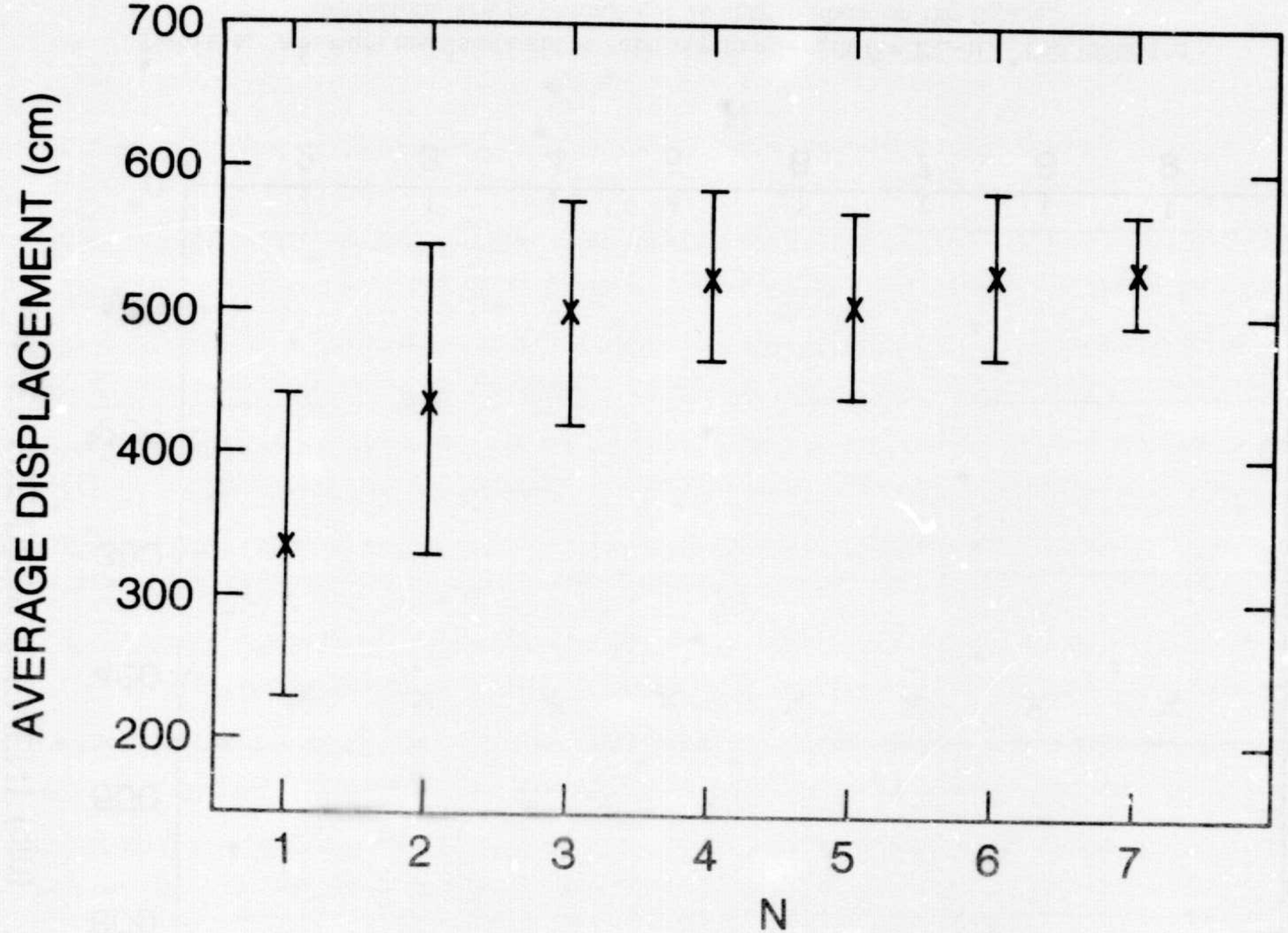

Figure 3. Average displacement versus rupture length for EL-I. The X's represent mean values and the bars show the range for one standard deviation about the mean.

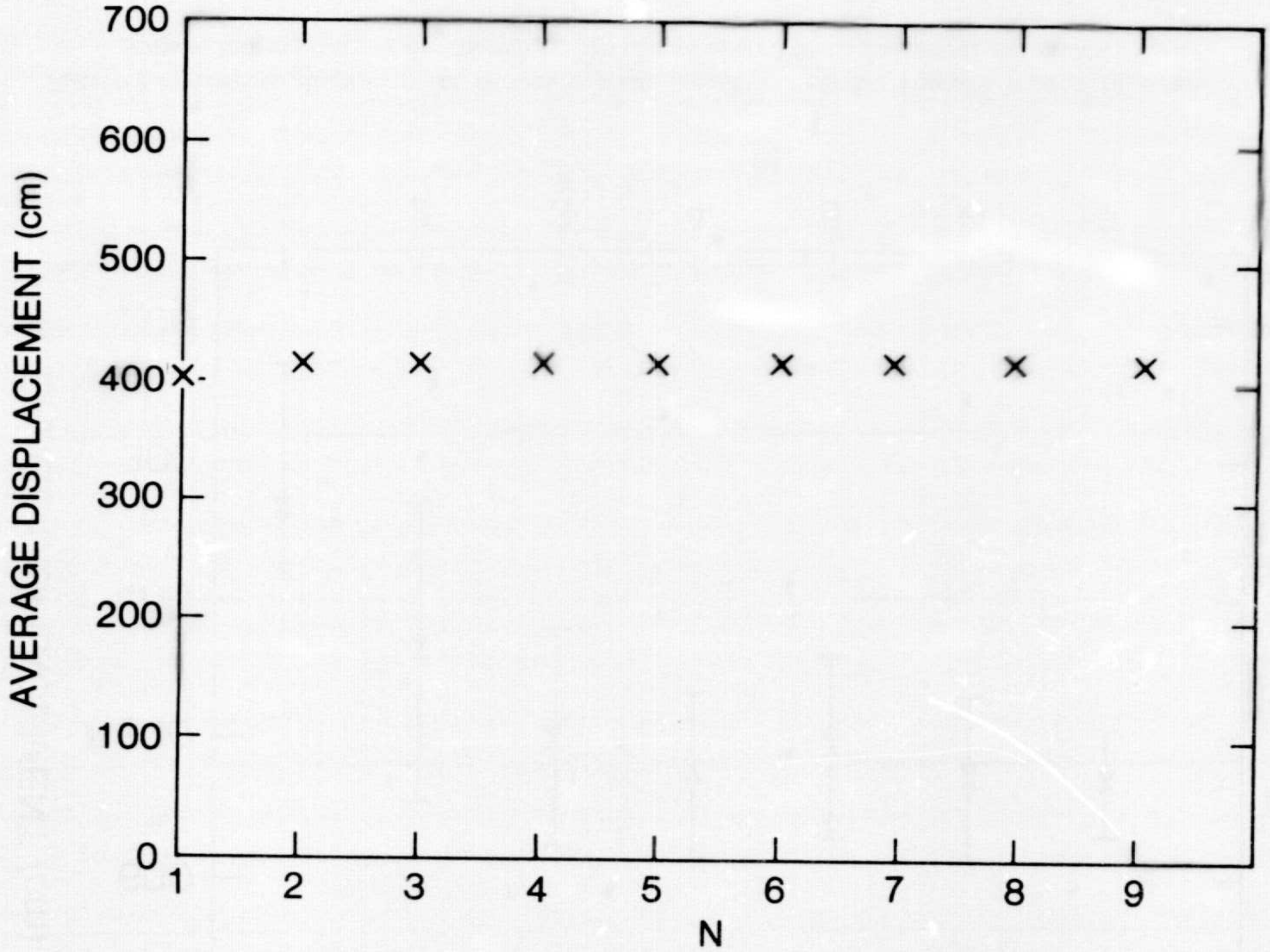

Figure 4. Average displacement versus rupture length for EL-II. The standard deviations are too small (< 10 cm) to show on the figure.

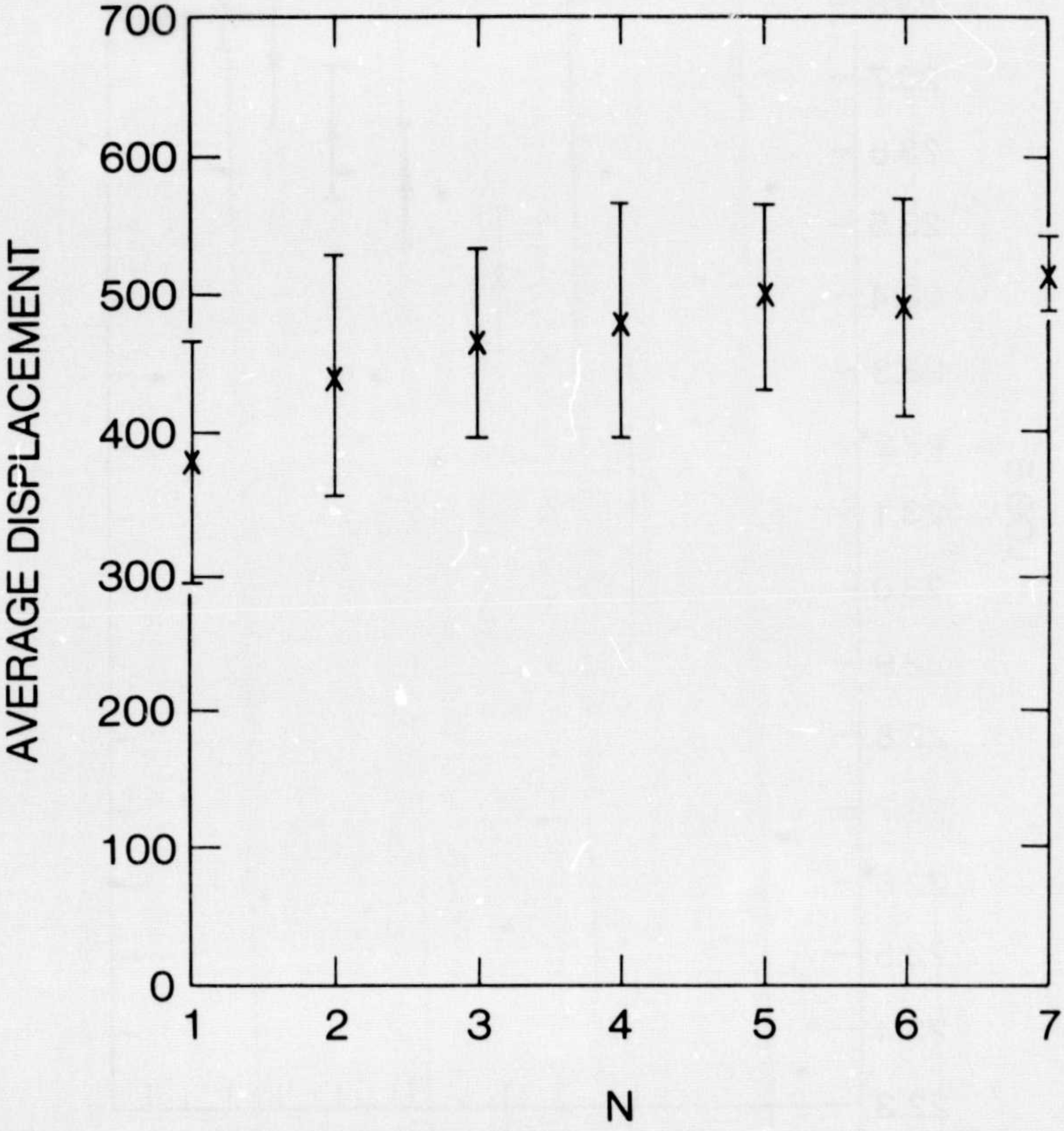

Figure 5. Average displacement versus rupture length for EL-III

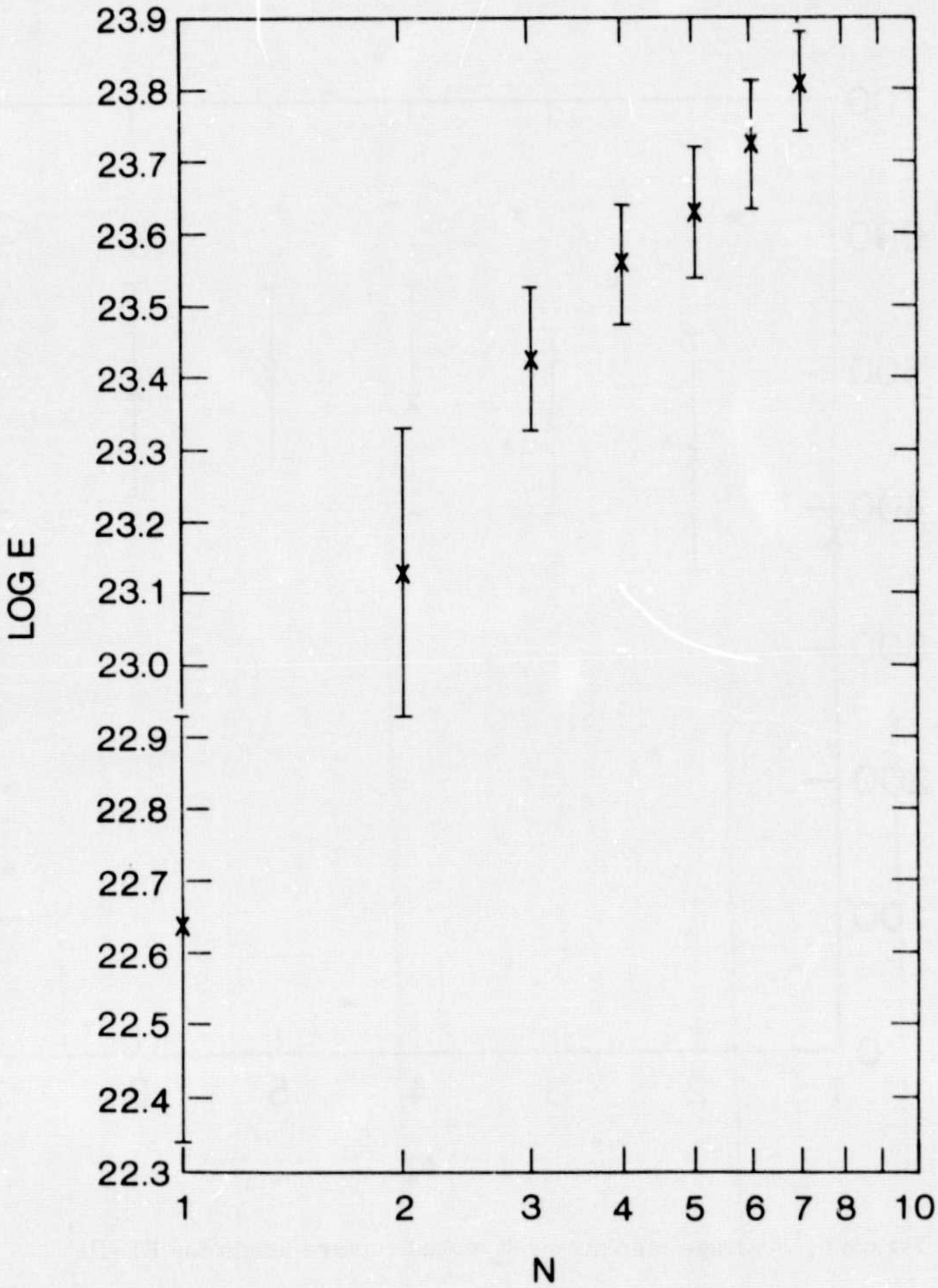

Figure 6. Energy versus rupture length for EL-I. The X's represent mean values of log E and the bars show the range for one standard deviation about the mean.

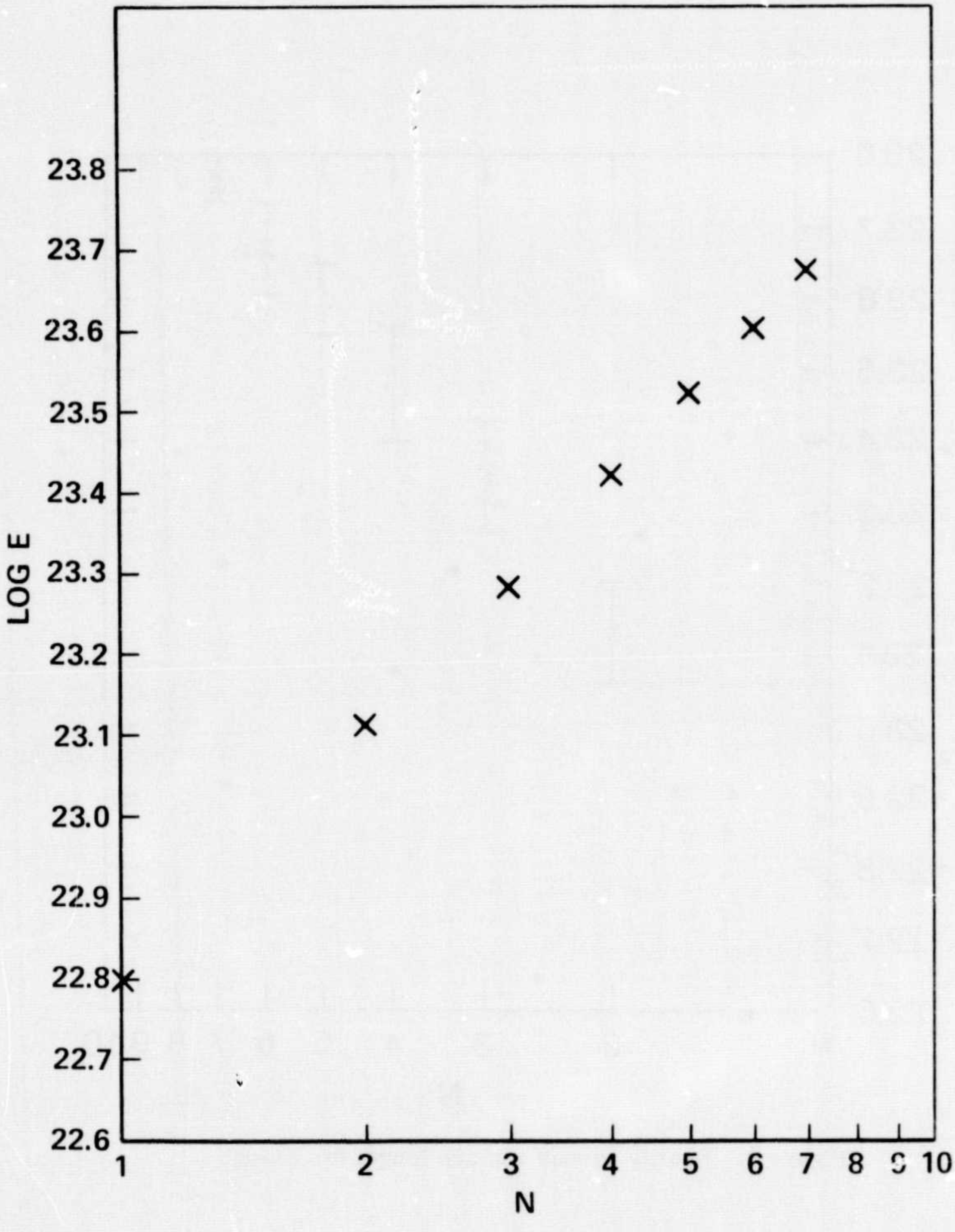

Figure 7. Energy versus rupture length for EL-II. The standard deviations are too small ($\leqslant 0.01$) to show on the figure.

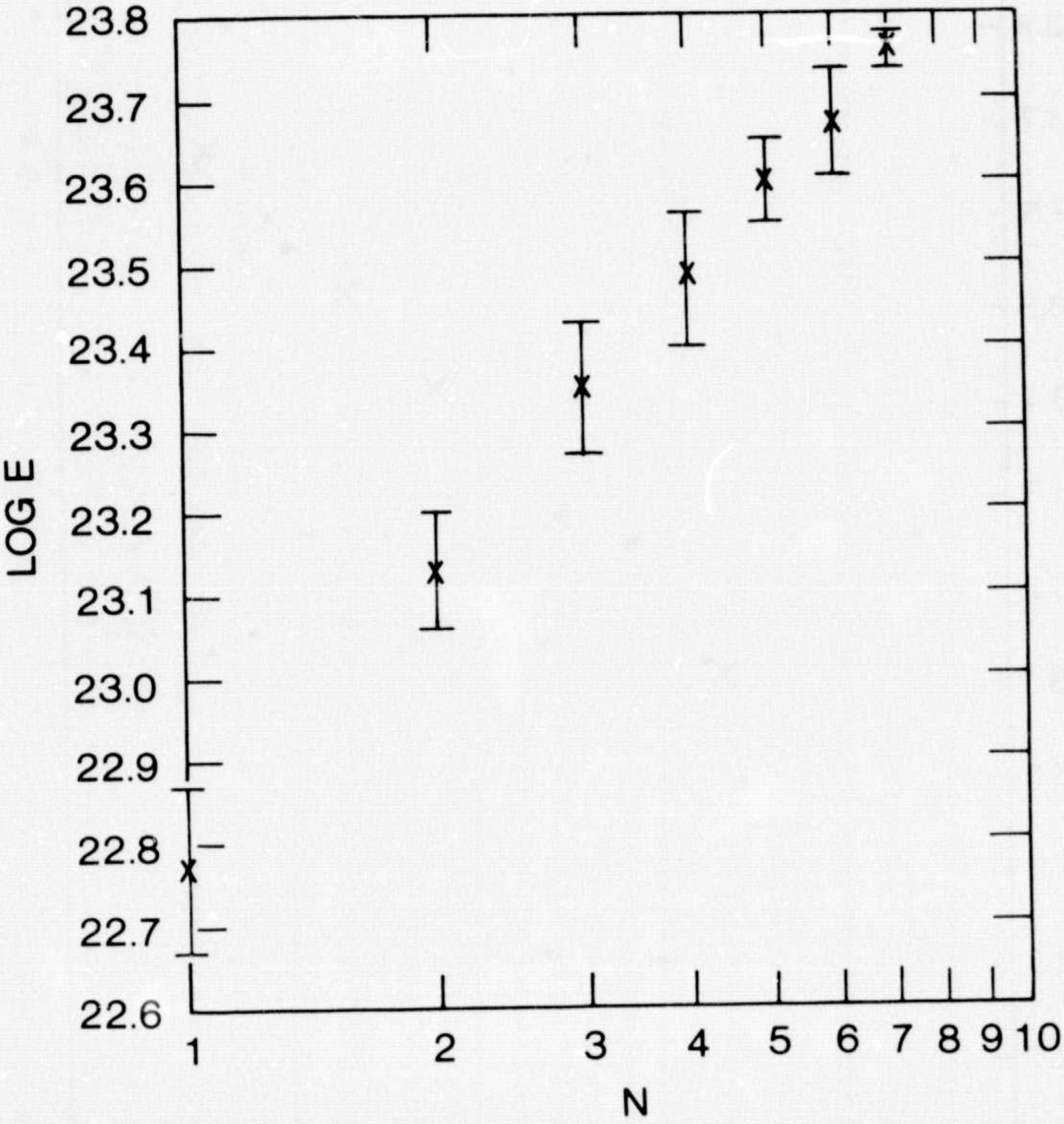

Figure 8. Energy versus rupture length for EL-III

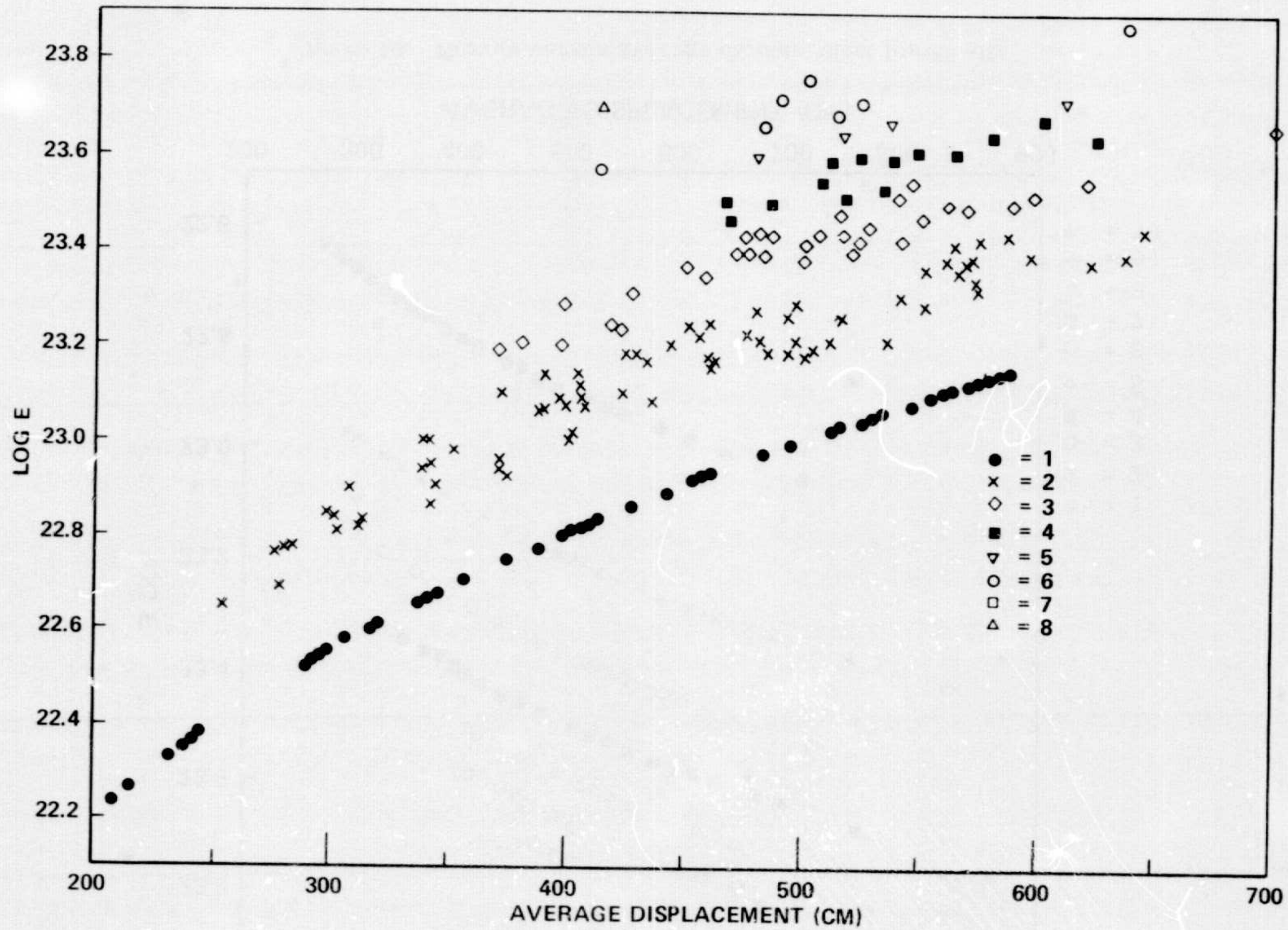

Figure 9. Energy versus average displacement for EL-I. Each point represents at least one event.

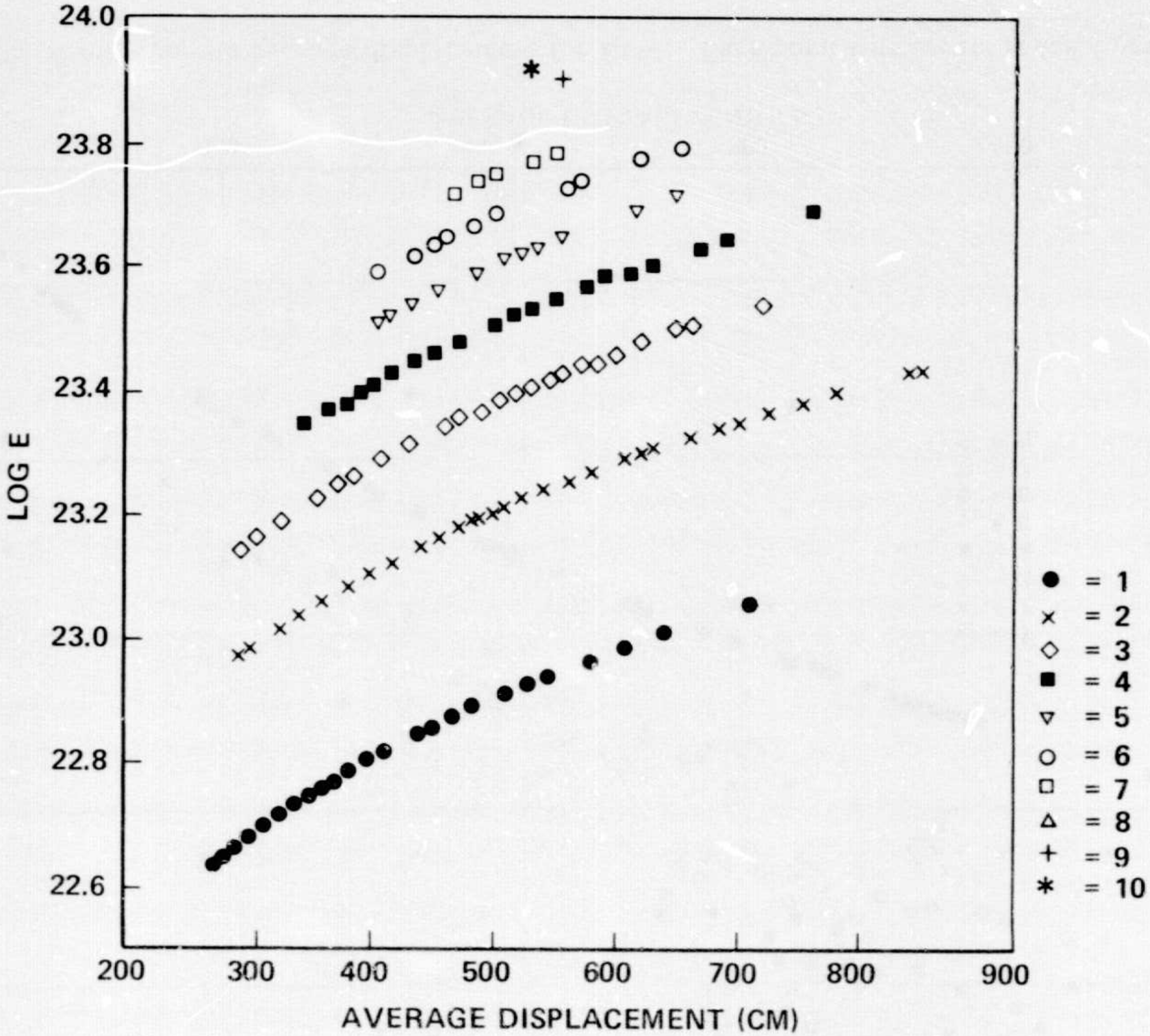

Figure 10. Energy versus average displacement for EL-III

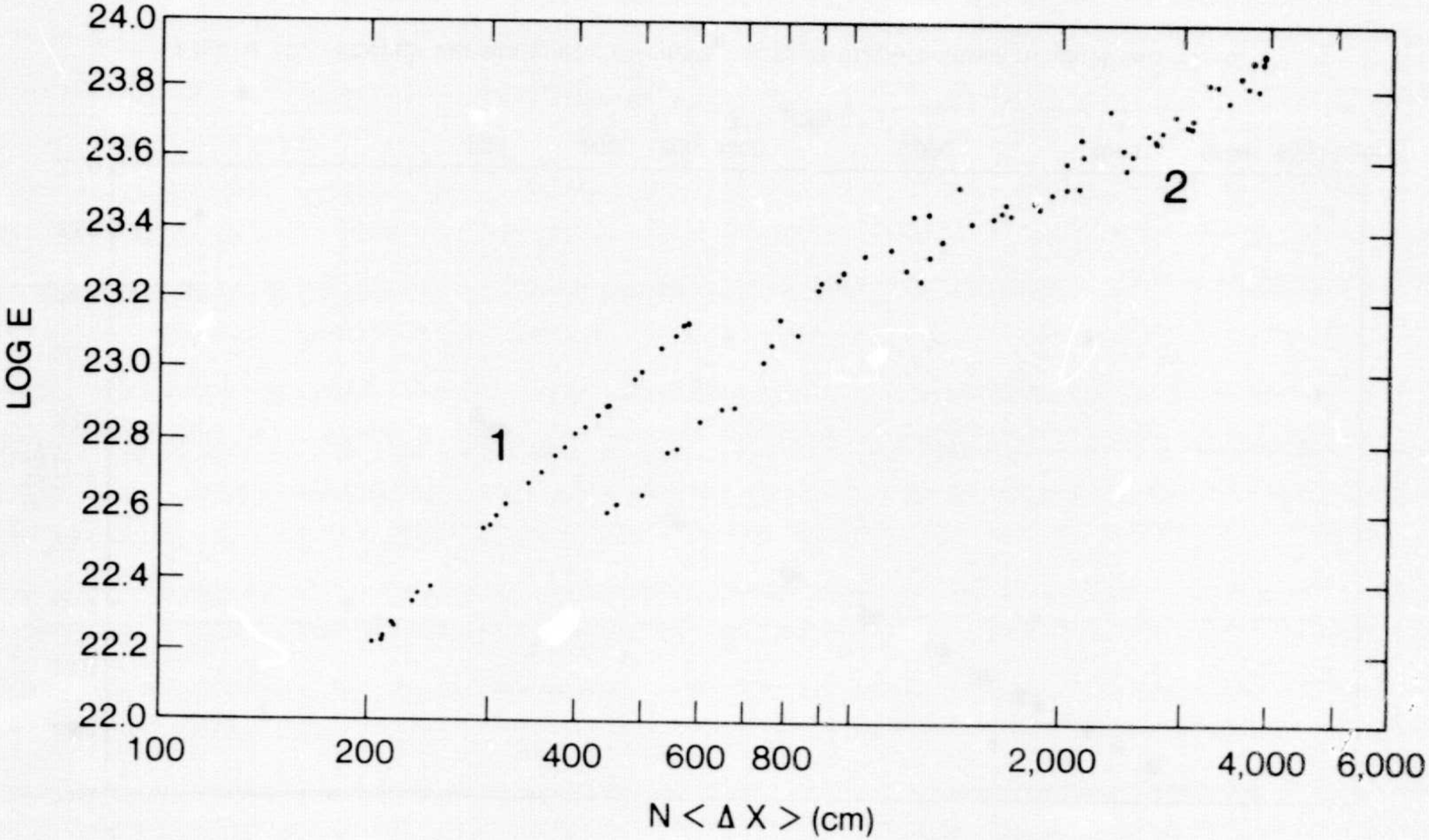

Figure 11. Energy versus rupture length-average displacement product for EL-I

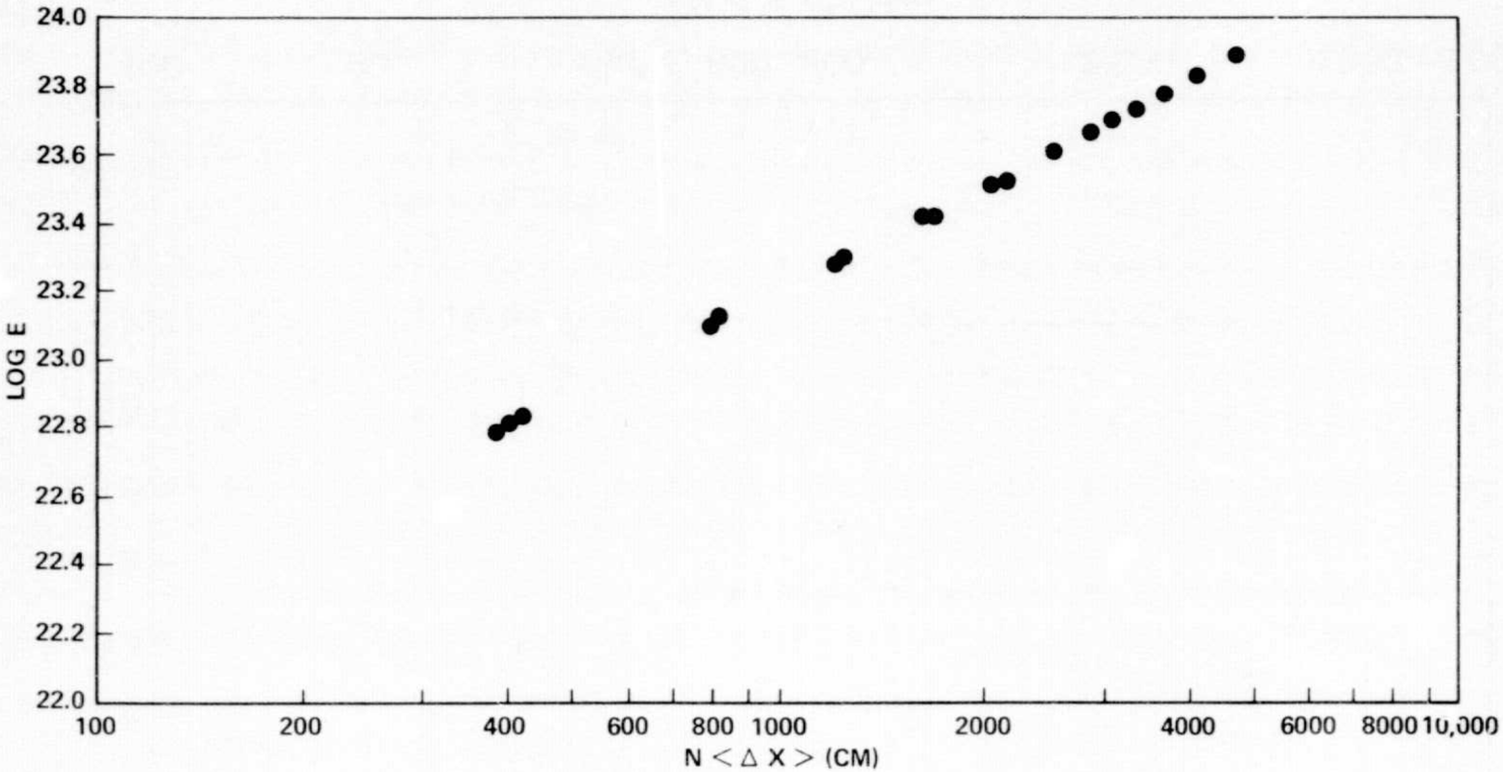

Figure 12. Energy versus rupture length-average displacement product for EL-II

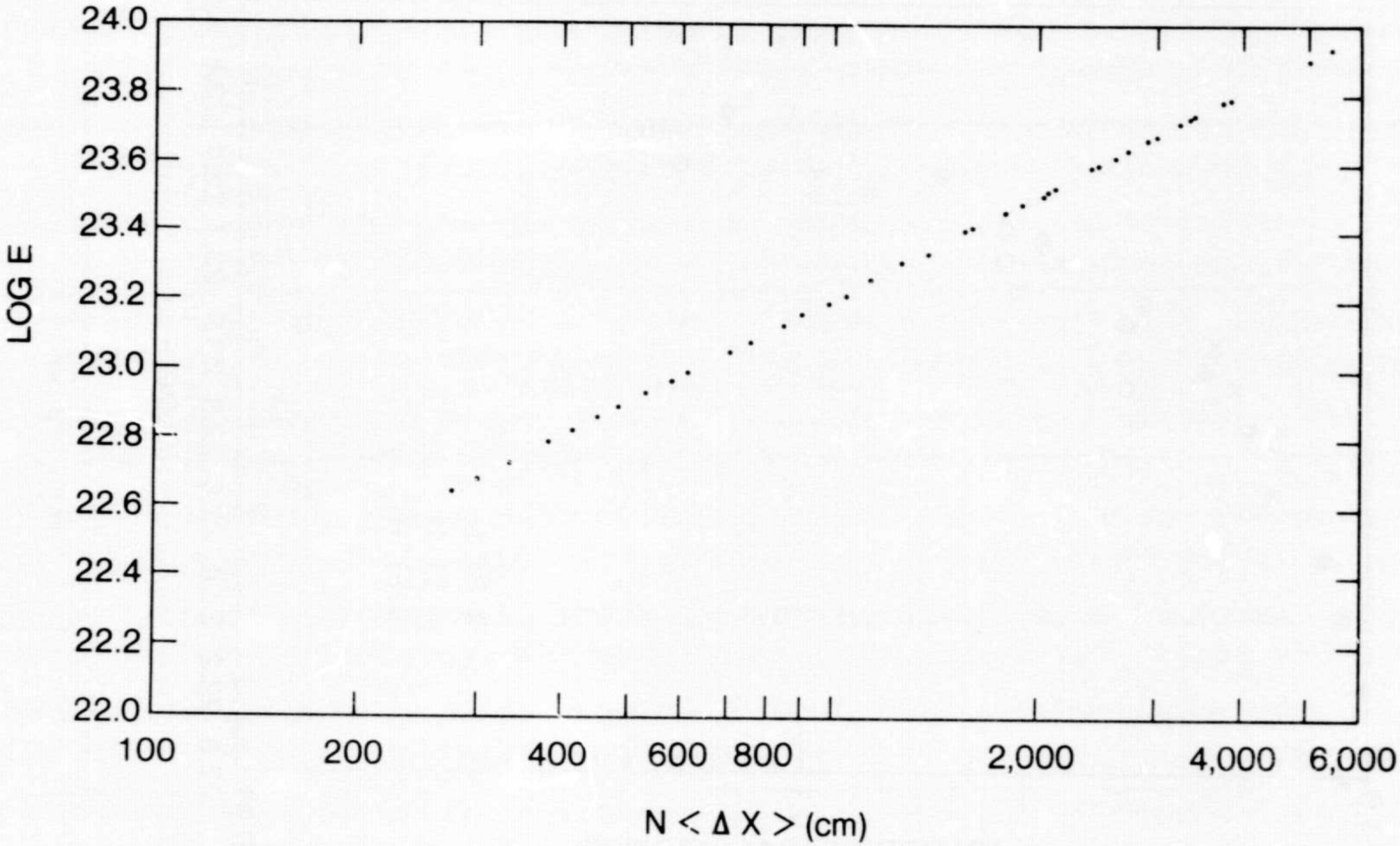

Figure 13. Energy versus rupture length-average displacement product for EL-III

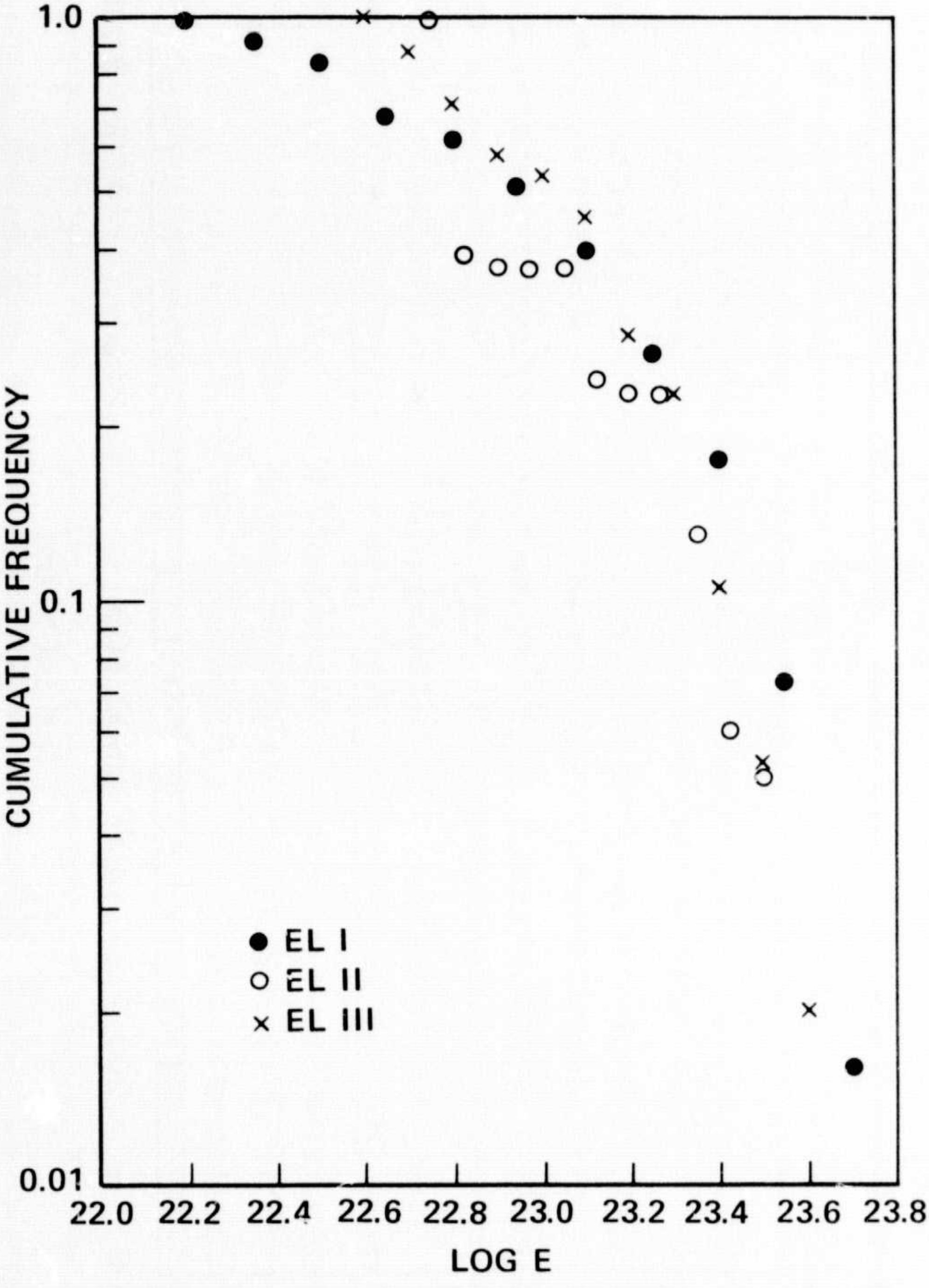

Figure 14. Fractional frequency of occurrence of events with energy ≤E versus E